Light-induced charge transport in $LiNbO_3$ crystals

B. Sturman,[1] M. Carrascosa,[2] and F. Agullo-Lopez[2]
[1]*Institute of Automation and Electrometry, Russian Academy of Sciences, 630090 Novosibirsk, Russia*
[2]*Universidad Autonoma de Madrid, Campus de Cantoblanco, E-28049 Madrid, Spain*
(Received 26 August 2008; revised manuscript received 4 November 2008; published 17 December 2008)

We develop a concept of charge transport for congruent and stoichiometric $LiNbO_3$ crystals, both doped and nominally pure. The concept is based on well-established experimental facts. It incorporates fragments of the known one-center and two-center models and other important elements including electronic transitions and transport channels. The model explains qualitatively the main features of the optical damage for the congruent and stoichiometric compositions within the low-to-high intensity range.

DOI: 10.1103/PhysRevB.78.245114 PACS number(s): 72.20.Jv, 78.20.Bh, 42.70.Nq

I. INTRODUCTION

The long-standing problem of light-induced charge transport in lithium niobate ($LiNbO_3$) and lithium tantalate ($LiTaO_3$) crystals can be formulated as follows. What is the reason for the generation of the anomalously large steady-state photovoltaic electric fields, $E_{pv} \approx 10^5$ V/cm or even higher, in the illuminated area? What are the main factors affecting these fields? How to control them? What makes a difference with many other materials possessing modest or low photovoltaic fields?

The problem dates back from 1966 when the photorefractive effect was detected,[1] and it has been under purposeful study since 1974 when the bulk photovoltaic effect was discovered.[2] It is far from trivial already because of the complexity of the charge transport in ionic wide-gap crystals. It is closely related to the photorefractive studies because the light-induced fields produce the refractive index changes via the linear electro-optic effect.[3] Lastly, it is crucial for numerous nonphotorefractive applications of $LiNbO_3$ crystals involving the electro-optic properties, the periodical poling, the second-harmonic generation, etc.[4–7] because the light-induced fields cause strong optical damage.

In the low-intensity range, $I \lesssim 1$ W/cm^2, the main facts for Fe-doped and Cu-doped crystals were interpreted within a one-center model by the end of the 1980s.[8] This implies that electrons are photoexcited from deep Fe^{2+} (Cu^+) centers into the conduction band (CB) and recombine directly to the empty Fe^{3+} (Cu^{2+}) centers. The photovoltaic length (the mean electron displacement per absorbed photon) was found to be comparable with that in many other photovoltaic materials, $l^* \approx 1$ Å, while the mobility-lifetime product for CB electrons, which is the measure of the photoconductivity, was found to be extremely small for modestly doped samples, $\mu\tau \approx 10^{-13}$ cm^2/V, causing anomalously large photovoltaic fields $E_{pv} = l^*/\mu\tau$.[8–11]

The measured ultrasmall values of the $\mu\tau$ product are extremely challenging within the one-center model. With the minimum value of the band mobility admitted for the delocalized electrons, $\mu \approx 1$ cm^2/Vs,[12] the recombination time τ must be of the order of 10^{-13} s. This is three to four orders of magnitude shorter than the times typical for allowed recombination transitions and comparable with the time of interband energy relaxation.[13,14] It is unlikely that admission of localized electrons in CB (owing to, e.g., the polaron effect) can solve the problem charge transport. The time of recombination to the deep centers is dramatically increasing for hopping electrons in this case because of the tunneling bottleneck, while the experimental value $l^* \approx 1$ Å becomes very difficult to explain.[10,11]

In 1993, the one-center model was extended for $LiNbO_3$:Fe crystals to explain the increasing absorption and index changes for sufficiently large intensities, $I \gtrsim 10^3$ W/cm^2.[15] An intermediate energy level was added to the energy scheme and a few additional channels of photoexcitation and recombination were taken into account; the recombination channel from CB to the intermediate level was discarded. In the low-intensity range, the above two-center model transfers to the one-center one so that the problem of extremely small values of the $\mu\tau$ product remains untouched. The latest developments of the two-center model can be found in Refs. 16 and 17. They are also focused on the high-intensity range.

In the beginning of the 1990s, the relatively shallow levels attributed to the intrinsic defects Nb_{Li} (also called antisite defects and bound polarons) attracted great attention.[18–21] The point is that the previously investigated $LiNbO_3$ crystals were predominantly congruent [congruent lithium niobate (CLN)]. They possessed a considerable lithium deficit, and correspondingly, a big amount ($\approx 10^{20}$ cm^{-3}) of the intrinsic antisite defects. The technological progress has allowed one to grow near-stoichiometric lithium niobate (SLN), where the concentration of the antisite defects is reduced by approximately two orders of magnitude.[20] Many physical properties of the SLN, including the ferroelectric and photorefractive, were found to be improved compared to those of the CLN. In particular, the undoped SLN is more resistant to the optical damage, and the photorefractive properties of the CLN and SLN crystals are different in the low-intensity range.[20,21]

Further progress was made with pulse measurements. In experiments with picosecond pump pulses at 532 nm, it was found that the shallow Nb_{Li} levels become populated after the excitation of electrons from deep Fe^{2+} levels to the CB, which causes a considerable red and near-infrared absorption.[22,23] The lifetime of electrons on the Nb_{Li} sites turned out to be pretty long; it ranged from ≈ 1 to 10^3 μs depending on the crystal composition and doping level. The recombination was not monoexponential but stretched expo-

nential, which strongly indicates involvement of hopping or tunneling processes. Similar observations of the long-term relaxation in $LiNbO_3$ crystals were reported in a close relation to the two-color hologram recording.[24] Recent experiments with femtosecond pulses have shown that the population of the Nb_{Li} levels after a two-photon excitation of undoped CLN crystals occurs very quickly, faster than 10^{-13} s.[25–27]

As it is clear from the accumulated evidences, the charge transport model for $LiNbO_3$ crystals has to be revisited to incorporate properly the impact of the intermediate Nb_{Li} centers and to analyze the dependence of the light-induced fields not only on the concentration of deep centers, such as Fe or Cu, but also on the density of the antisite defects. In other words, close attention has to be paid to both CLN and SLN crystals. Furthermore, both the low-intensity and high-intensity ranges are of great importance.

This paper is an attempt to refine the physical picture of light-induced charge transport in CLN and SLN crystals, to describe, at least qualitatively, the main accumulated experimental facts, and to make predictions. Being essentially different from the previous models, our theory keeps their important features which are relevant to the high-intensity range.

We will assume that the concentration of the antisite defects is much larger than the concentration of deep traps. We thus pretend to cover the cases of undoped and modestly doped CLN crystals and also the case of undoped SLN crystals. The cases of heavily doped CLN and doped SLN are beyond our study. Some additional assumptions will be introduced and justified during the course of our considerations.

Some complicating circumstances have to be mentioned to clarify the physical background. The concentration of the antisite defects can usually be estimated only approximately. The light absorption coefficient and the concentration of deep traps in undoped samples are very difficult to measure. In this connection, the experimental data on the optical damage remain often incomplete—only the threshold light intensities are available.

II. BASIC MODEL

A. Excitation and recombination channels

The energy scheme and the main transitions are shown in Fig. 1. The total concentrations of the deep (0) and intermediate (1) centers are N_0 and N_1, while the concentrations of electrons occupying the levels 0, 1, and 2 (CB) are n_0, n_1, and n_2, respectively. The total concentration of electrons $n_t = n_0 + n_1 + n_2$ can be treated as a conserving quantity for uniform and quasiuniform illumination. Initially, all electrons occupy the ground level 0. According to our main assumption, we have $N_0 \ll N_1$. Additionally, we accept for simplicity that $n_t \ll N_0$; this condition is usually satisfied in $LiNbO_3$ crystals doped with Fe or Cu. Generalization to the case $N_0 - n_t \lesssim N_0$ should present no problems.

Two main channels of the photoexcitation are 02 and 12, which are shown by the upward arrows. Apparently, the channel 12 is important only for sufficiently large intensities;

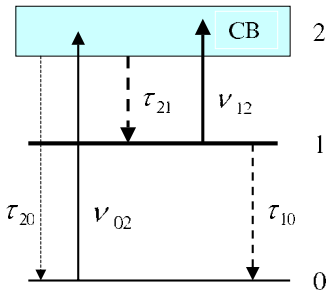

FIG. 1. (Color online) Scheme of the energy levels and main electronic transitions.

it is generic for all two-center models of charge transport in lithium niobate. The strongest recombination channel for the CB is 21; it corresponds to the shortest recombination time $\tau_{21} \propto N_1^{-1}$. This channel was discarded in Ref. 15. The recombination channel 20, which is characterized by the time $\tau_{20} \propto N_0^{-1}$ and can generally compete with the channel 21, is expected to be negligible. The corresponding condition $\tau_{21} \ll \tau_{20}$ can be easily justified. (i) The number of shallow traps N_1 is the largest and the energy distance from them is the smallest. (ii) Ultrafast recombination to the antisite defects has been proven experimentally.[25–27] The bottleneck of the recombination process in our model is the channel 10 with the longest recombination time τ_{10}. This channel implies electronic tunneling transitions between the localized states; it will be considered in detail in Sec. IV.

With the priority of the recombination channel 21 over 20 established, it becomes clear why the excitation channel 01 can be discarded: This channel is merely much weaker than the band excitation channel 02 that provides (via the strong 21 recombination channel) a very efficient occupation of the intermediate level 1. Taking the excitation channel 01 into account would give only minor corrections to the concentrations $n_{0,1,2}$.

Note that the thermal excitation of electrons into the CB is discarded in our model. In Refs. 16, 17, and 28, where the recombination channel 10 is neglected, the thermal excitation channel 12 provided the only possibility for electrons at the intermediate level 1 to recombine to the ground state. Unfortunately, this scheme gives no real advantages for explanation of the anomalously small values of the $\mu\tau$ product—the steady-state value of n is controlled again by the time τ_{20} and does not depend on τ_{21}. In our scheme, the thermal excitation channel 12, if efficient, would give only minor corrections to the electron concentrations in the high-intensity range.

The simplest balance equations for our two-center model are

$$\dot{n}_2 = \nu_{02} I n_0 + \nu_{12} I n_1 - \tau_{21}^{-1} n_2, \tag{1}$$

$$\dot{n}_1 = \tau_{21}^{-1} n_2 - \tau_{10}^{-1} n_1 - \nu_{12} I n_1, \tag{2}$$

where I is the light intensity, $\nu_{02} = \sigma_{02}/\hbar\omega$, $\nu_{12} = \sigma_{12}/\hbar\omega$, $\hbar\omega$ is the energy of a light quantum, and σ_{02} and σ_{12} are the excitation cross sections. Since $n_t = n_0 + n_1 + n_2 = \text{constant}$,

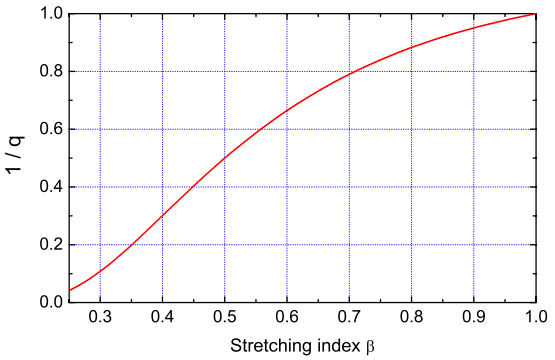

FIG. 2. (Color online) Correction factor $1/q$ versus the stretching index β.

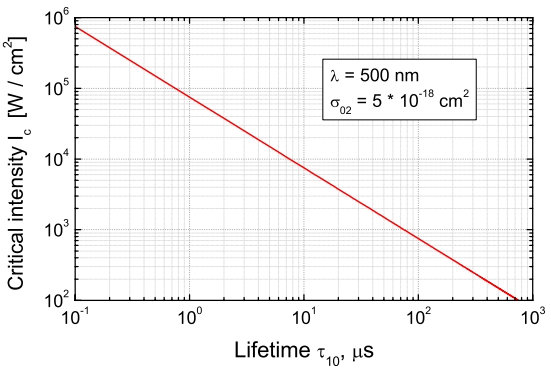

FIG. 3. (Color online) Critical intensity I_c versus the lifetime for level 1.

these two equations are sufficient to find the electron concentrations $n_{0,1,2}$.

It is worthy of mentioning that the term $\tau_{10}^{-1}n_1$ in Eq. (2) does not describe the stretched-exponential relaxation which occurs for the channel 10. To include this relaxation into our theory, this term has to be replaced by a more general one, $\int_0^\infty n_1(t-t')f(t')dt'$, where the positive function $f(t')$ tends to 0 for $t\to\infty$. The structure of this term is dictated by the causality principle and by the linearity of the recombination process. The function $f(t')$ has to be chosen in such a way to ensure the decay law $n_1/n_1(0)=\exp[-(t/\tau_{10})^\beta]$ in the absence of the excitation.

As shown in the Appendix, in steady state this generalization leads to a simple renormalization, $\tau_{10}\to q\tau_{10}$, where q is a function of the stretching index β shown in Fig. 2. Typically, $\beta=(0.3-0.6)$ in the experiments so that the influence of this renormalization is modest. Furthermore, it does not affect the character of the intensity dependences.

B. Low-intensity and high-intensity ranges

In the low-intensity range, the excitation channel 12 can be neglected. It is evident that we have here $n_0/n_t\simeq 1$, $n_2/n_t\simeq\nu_{02}I\tau_{21}$, and $n_1/n_2=\tau_{10}/\tau_{21}\gg 1$ in steady state. In other words, the concentration of electrons in the CB is controlled by the shortest recombination time τ_{21} and has nothing to do with the much longer times τ_{20} and τ_{10}. We have thus an effective one-center model for CB. At the same time, the photoexcited electrons are accumulating on the metastable level 1; their concentration is determined by the longest time τ_{10}.

If the cross sections σ_{02} and σ_{12} are of the same order of magnitude (which will be expected in what follows), the low-intensity case is restricted by the inequality $I\lesssim I_c$, where

$$I_c=\frac{1}{\nu_{02}\tau_{10}}=\frac{\hbar\omega}{\sigma_{02}\tau_{10}} \tag{3}$$

is the critical intensity. It is controlled by the longest recombination time τ_{10}.

It is instructive to consider I_c as a function of time τ_{10}. Figure 3 gives this dependence for $\lambda=500$ nm and $\sigma_{02}=5\times 10^{-18}$ cm^2, which is representative of Fe^{2+} centers. The range of τ_{10} corresponds roughly to the literature data.[20,22,24] The smallest values of I_c are expected for SLN crystals. For the CLN samples the low-intensity range is much wider.

The steady-state solution of Eqs. (1) and (2), which is applicable to the whole actual intensity range, can be presented in a simple form,

$$\frac{n_0}{n_t}\simeq\frac{1}{1+x},$$

$$\frac{n_1}{n_t}\simeq\frac{x}{1+x},$$

$$\frac{n_2}{n_t}\simeq\frac{ax(1+bx)}{1+x}, \tag{4}$$

where $x=I/I_c$, $a=\tau_{21}/\tau_{10}\ll 1$, and $b=\nu_{12}/\nu_{02}\equiv\sigma_{12}/\sigma_{02}\sim 1$ are useful dimensionless parameters. For $x\ll 1$ we return to the low-intensity range. In the opposite limit, $x\gg 1$, we have $n_0/n_t\ll 1$, $n_1/n_t\simeq 1$, and $n_2/n_t\simeq abx=\nu_{12}I\tau_{21}\ll 1$. Obviously, the last two relations correspond to the one-center model where the level 1 plays the role of the ground levels and $n_2\propto I$. Only the excitation rate for the CB is modified, $\nu_{12}\neq\nu_{02}$. The only restriction from above on the light intensity is $\nu_{02}I\tau_{21}\ll 1$; since $\tau_{21}\ll\tau_{10}$, it is very soft, which means that the transition 02 is not saturated.

C. Diffusion-controlled recombination 1→0

The recombination time τ_{10} was treated above as a model parameter. It is important to clarify its meaning. Since $N_1\gg N_0$, the mean distance between two neighboring shallow center 1's, $\bar{R}_1\approx N_1^{-1/3}$, is noticeably shorter than the mean distance between the deep centers, $\bar{R}_0\approx N_0^{-1/3}$, and also than the mean distance between centers 1 and 0. The latter is about $\bar{R}_0$. Furthermore, the localization radius r_1 for electrons occupying center 1 is much smaller than $\bar{R}_1$, and the localization radius for electrons in the ground state r_0 is smaller than r_1.

We are dealing thus with a hopping process where the probability of a single hop (tunneling event) per second is exponentially small [proportional to the factor $\exp(-\bar{R}_1/r_1)$] because of a very small overlap of the wave functions for the

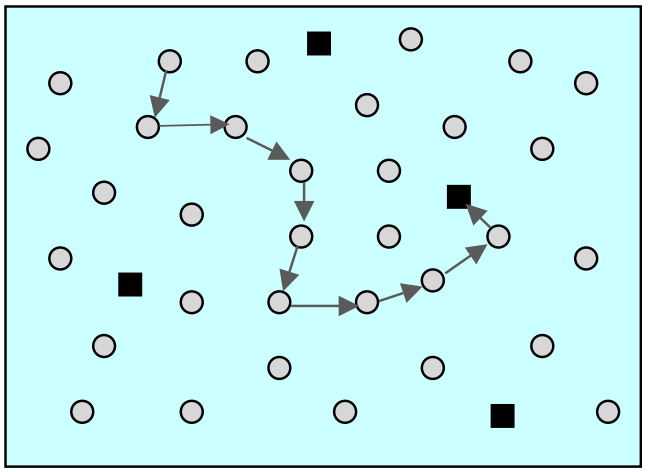

FIG. 4. (Color online) Migration of an electron over level 1 (gray circles) and recombination to the ground state 0 (black squares).

neighboring centers. This factor is sharply decreasing with increasing hopping distance $\bar{R}_1$. We denote the average hopping probability for center 1 as $W_1 = W_1(\bar{R}_1)$. Generally, it is also thermally activated because of the polaron effect. Particular expressions and numerical estimates for W_1 are model dependent and not very reliable. They are not really important for our theory.

The physical picture of recombination $1 \rightarrow 0$ can be presented as follows. An electron migrates (diffuses) by hops from one Nb_{Li} center to another until it approaches occasionally a deep recombination center 0. Only after that can a recombination event occur, see Fig. 4. Such a situation is typical for diffusion-controlled processes or reactions in solid states.[29] It leads often to stretched-exponential dynamics.[30] The diffusion coefficient D_1 for hopping migration over center 1 can roughly be estimated as $D_1 \approx W_1 \bar{R}_1^2 \approx W_1 N_1^{-2/3}$.

Let us estimate the lifetime of the metastable levels τ_{10}. It is evident that the fraction of migrating electrons that occupy positions nearby the recombination centers is proportional to N_0/N_1. Therefore, the rate of recombination from level 1 can be presented as $Cn_1 W_1 N_0/N_1$ so that the recombination time is given by

$$\tau_{10}^{-1} = C W_1 N_0 / N_1, \tag{5}$$

where C is a certain constant. Its value depends on the effective cross section of the recombination centers. When they are attractive, many positions around a single center are favorable for recombination and $C \gg 1$. We will treat C as a fit parameter. Dependence of τ_{10} on the concentration N_1 is unusual for the photorefractive band models.

III. OBSERVABLE CHARACTERISTICS

The main observable characteristics are the photoconductivity σ_{ph}, the photovoltaic current j_{pv}, the light-induced field E_{pv}, and the light absorption coefficient α. We calculate them below within the basic model.

A. Photoconductivity

Within our model, the initial expression for the photoconductivity is $\sigma_{ph} = e(\mu_1 n_1 + \mu_2 n_2)$, where μ_1 and μ_2 are the mobilities of electrons for levels 1 and 2 (CB), respectively. One of the most important outcomes of our model is that the first contribution, which is due to hopping over the antisite defects, cannot generally be neglected as compared to the conventional CB contribution.

The presence of a significant hopping contribution for a concentration of the antisite defects $N_1 \approx (10^{19}-10^{20})$ cm^{-3} cannot be surprising; in semiconductors the hopping conductivity becomes important even for much lower concentrations of impurities.[31] Furthermore, it is found for lithium niobate that the dark hopping conductivity owing to tunneling over deep Fe^{3+} centers becomes important for $N_{Fe} \gtrsim 10^{19}$ cm^{-3}.[32,33] Since electrons occupying the antisite defects are much less localized, their contribution to σ_{ph} must be taken into account.

Consider first the low-intensity range, $I \ll I_c$. Here we have $n_1 \approx n_t \nu_{02} \tau_{10}$ and $n_2 \approx n_t \nu_{02} \tau_{21}$ so that the mobility-lifetime products $\mu_1 \tau_{10}$ and $\mu_2 \tau_{21}$ are of prime importance. The mobility of electrons migrating over center 1 can be calculated from the Einstein relation, $\mu_1 = eD_1/k_B T$, where k_B is the Boltzmann constant and T is the absolute temperature. Using Eq. (5) and the above estimate of D_1, we obtain for the hopping-related product

$$\mu_1 \tau_{10} = \frac{e}{k_B T} \frac{N_1^{1/3}}{C N_0}. \tag{6}$$

This product *does not include* the hopping probability W_1 and the uncertainties related to modeling of this microscopic parameter. The estimate of $\mu_1 \tau_{10}$ is therefore more robust than that of τ_{10} and μ_1 separately.

The total photoconductivity in the low-intensity range is given by

$$\sigma_{ph} = e \nu_{02} n_t I (\mu_1 \tau_{10} + \mu_2 \tau_{21}). \tag{7}$$

The product $\nu_{02} n_t$ in this relation is $\alpha/\hbar\omega$, where α is the light absorption coefficient. It can be measured if the concentration of photoexcitable electrons n_t is big enough.

Which of the two contributions to σ_{ph} is the largest? The answer is important for the understanding of the photorefractive properties of lithium niobate. Obviously, only the ratio $\mu_2 \tau_{21}/\mu_1 \tau_{10}$ is important for comparison. It can generally be larger and smaller than 1 in different regions of N_0 and N_1 because the expected dependences $\mu_1 \tau_{10}(N_0, N_1)$ and $\mu_2 \tau_{21}(N_0, N_1)$ are different, see also Sec. IV.

Using Eq. (4), we can easily extend the above result for σ_{ph} to the whole intensity range,

$$\sigma_{ph} = \frac{e n_t I}{1 + I/I_c} [\mu_1 \tau_{10} \nu_{02} + \mu_2 \tau_{21} (\nu_{02} + \nu_{12} I/I_c)]. \tag{8}$$

For $I/I_c \ll 1$ we return to Eq. (7). For $I/I_c \gg 1$ we have

$$\sigma_{ph} \simeq e n_t (\mu_1 + \mu_2 \tau_{21} \nu_{12} I). \tag{9}$$

Since the value of μ_1 can be very small, the second term can easily become dominating for $I \gg I_c$.

B. Photovoltaic current

Modeling of the photovoltaic effect in lithium niobate is based on the widespread assumption that only the excitation asymmetry matters. With this assumption, the excitation channels 02 and 12 possess generally different photovoltaic lengths l_{02}^* and l_{12}^*. Employing the starting expression $j_{pv}=eI(\nu_{02}n_0l_{02}^*+\nu_{12}n_1l_{12}^*)$ for the photovoltaic current and using Eq. (4), we obtain in the whole intensity range

$$j_{pv}=\frac{en_tI}{1+I/I_c}(\nu_{02}l_{02}^*+\nu_{12}l_{12}^*I/I_c). \tag{10}$$

For $I\ll I_c$, we have $j_{pv}\simeq eI\nu_{02}n_tl_{02}^*$, while in the opposite case, $I\gg I_c$, Eq. (10) gives a new linear dependence $j_{pv}\simeq eIn_t\nu_{12}l_{12}^*$.

C. Light-induced field

Combining Eqs. (8) and (10), we obtain for the steady-state photovoltaic field $E_{pv}=j_{pv}/\sigma_{ph}$

$$E_{pv}=\frac{\nu_{02}l_{02}^*+\nu_{12}l_{12}^*I/I_c}{\mu_1\tau_{10}\nu_{02}+\mu_2\tau_{21}(\nu_{02}+\nu_{12}I/I_c)}. \tag{11}$$

In the low-intensity limit it gives

$$E_{pv}=\frac{l_{02}^*}{\mu_1\tau_{10}+\mu_2\tau_{21}}, \tag{12}$$

whereas for $I\gg I_c$, we have

$$E_{pv}=\frac{l_{12}^*}{\mu_2\tau_{21}}. \tag{13}$$

In the high-intensity region, the field is determined only by the characteristics of the 12 and 21 transitions; in particular, it grows with increasing N_1. It is expected that $l_{12}^*>l_{02}^*$. Therefore, $E_{pv}(I)$ is a monotonously growing function.

D. Absorption coefficient

In our model, the light absorption coefficient is generally given by $\alpha=n_0\sigma_{02}+n_1\sigma_{12}$, and its ground value is $\alpha_0=n_t\sigma_{02}$. Therefore, we have for the whole intensity range

$$\frac{\alpha}{\alpha_0}=\frac{1+(\sigma_{12}/\sigma_{21})I/I_c}{1+I/I_c}, \tag{14}$$

which might be expected. The absorption coefficient α ranges from $\nu_{02}n_t$ for $I\ll I_c$ to $\nu_{12}n_t$ for $I\gg I_c$.

E. Refractive index changes

With a known value of the photovoltaic field E_{pv}, the refractive index change is given by $\Delta n=-n^3rE_{pv}/2$, where n is the background index and r is the relevant electro-optic coefficient. For the case of the extraordinary (e) polarization we have $n=n_e$ and $r=r_{33}$ while for the ordinary (o) polarization $n=n_0$ and $r=r_{13}$. The wavelength dependences of these quantities are tabulated.

IV. NUMERICAL EXAMPLES

Let us make first some realistic assumptions about the numerical values of the model parameters on the basis of available experimental data. Consider first CLN:Fe crystals and set $N_1=10^{20}$ cm^{-3} as the representative concentration of the antisite defects.[19,20,22] In the low-intensity range, the ratio $\sigma_{ph}/e\nu_{02}n_tI$ (i.e., the sum $\mu_1\tau_{10}+\mu_2\tau_{21}$ in our model) can roughly be estimated as $\approx 10^{-13}$ cm^2/V for $N_0=10^{19}$ cm^{-3}. With the experimental justified value $l_{02}^*\approx 1$ Å,[8,10,33] it gives the field $E_{pv}\approx 10^5$ V/cm and the index change $\Delta n_e\approx 10^{-3}$. Let us set now $\mu_2\tau_{21}=\mu_1\tau_{10}=10^{-13}$ cm^2/V for the chosen concentrations. This means, in particular, that the constant $C\approx 180$ according to Eq. (6). Considerably larger values of $\mu_1\tau_{10}$ and $\mu_2\tau_{21}$ would not be consistent with the measured large values of E_{pv}. Noticeably smaller values of $\mu_1\tau_{10}$ would lead to even larger estimates for C; for $C\approx 1$ the hopping transport over level 1 would be too strong. Much smaller values of the band-related product $\mu_2\tau_{21}$ would lead to discarded band transport.

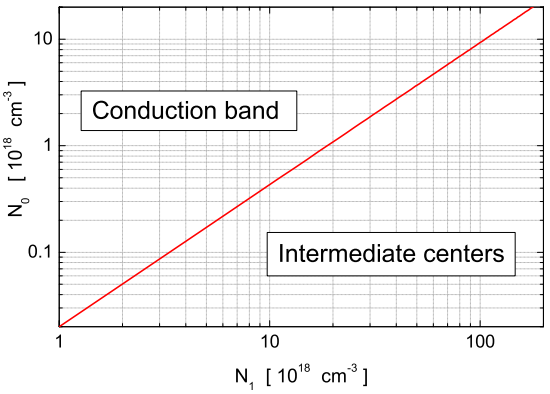

FIG. 5. (Color online) The line of equal contributions to the photoconductivity coming from CB and level 1. Above and below this line σ_{ph} is dominated by the CB and antisite defects (hopping contribution).

With the constant C estimated, we can analyze the dependence of the light-induced field on the degree of stoichiometry and concentration of deep centers in the low-intensity range. The following practical relation comes from Eq. (12):

$$\tilde{E}_{pv}=\frac{\tilde{N}_0\tilde{N}_1}{\tilde{N}_0+0.02\tilde{N}_1^{4/3}}. \tag{15}$$

Here $\tilde{E}_{pv}$ is the field E_{pv} measured in kV/cm, while $\tilde{N}_{0,1}$ are the concentrations $N_{0,1}$ measured in 10^{18} cm^{-3}.

Using this relation, we plot first the line $\tilde{N}_0=0.02\tilde{N}_1^{4/3}$ on the $\tilde{N}_1,\tilde{N}_0$ plane, see Fig. 5. In the regions above and below this line, the main contributions to the photoconductivity σ_{ph} come from the conduction band and intermediate centers, respectively. In particular, the hopping contribution via the intermediate levels dominates for weakly doped CLN crystals. For the SLN crystals the situation is different—both contributions can be important here depending on the particular choice of N_0 and N_1.

Figure 6 shows the dependence of E_{pv} on the concentration of deep traps N_0 in CLN crystals for three representative values of the concentration of the antisite defects N_1. It is linearly growing for sufficiently low values of N_0, $\lesssim 3\times 10^{18}$ cm^{-3}, and then tend to saturate. This behavior is con-

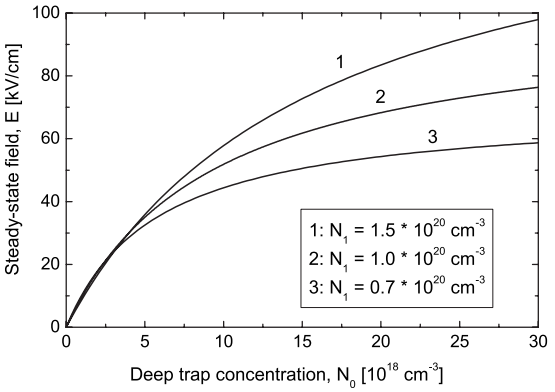

FIG. 6. Dependence $E_{pv}(N_0)$; curves 1, 2, and 3 are plotted for $N_1=1.5$, 1.0, and 0.7×10^{20} cm^{-3}, respectively.

sistent with experiments on iron-doped and copper-doped CLN crystals.[33,34]

Figure 7 exhibits the expected dependence of E_{pv} on the degree of stoichiometry N_1 for three small values of the deep trap concentration N_0, which are representative for undoped crystals. It shows that the SLN crystals possess generally larger photorefraction compared to the CLN ones. This is again in a qualitative agreement with experimental data.[35–38] The model predicts also that the function $E_{pv}(N_1)$ experiences a maximum in the region of small concentrations.

Consider now the main tendencies of the intensity dependence of the light-induced field. To plot $E_{pv}(I)$ we set additionally $I_{12}^*/I_{02}^*=3$ and $\sigma_{12}/\sigma_{02}=2$, which is in line with the previous theoretical studies. Figure 8 shows the dependence $E(I)$ for four representative concentrations of N_0 and N_1.

Curve 1 is plotted for $N_0=10^{19}$ cm^{-3} and $N_1=10^{20}$ cm^{-3}, which corresponds to doped CLN:Fe. Transition to the high-intensity region is expected here for $I_c\approx10^4$ W/cm^2 and the limiting value of E_{pv} is very high. Curve 2 corresponds to $N_0=10^{18}$ cm^{-3} and $N_1=10^{19}$ cm^{-3}; the doping level is modest and the stoichiometry is better here. Correspondingly, the critical intensity is lower ($I_c\approx10^3$ W/cm^2) as well as the limiting value of E_{pv}. Curve 3 is plotted for $N_0=10^{17}$ cm^{-3} and $N_1=10^{20}$ cm^{-3}; this is the case of weakly doped CLN:Fe. The limiting field is also very high here but the critical intensity is pretty low, $I_c\approx10^2$ W/cm^2. Lastly, curve

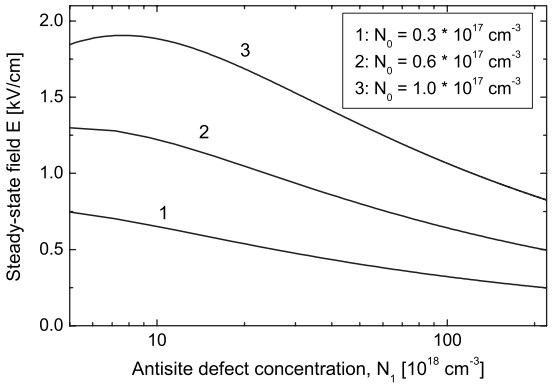

FIG. 7. Dependence $E_{pv}(N_1)$ for nominally undoped crystals. Lines 1, 2, and 3 are plotted for $N_0=0.3$, 0.6, and 1.0×10^{17} cm^{-3}, respectively.

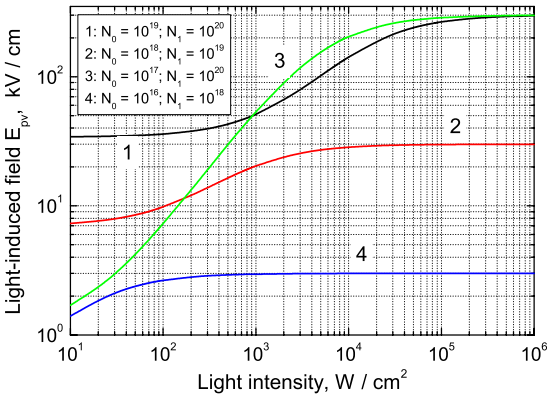

FIG. 8. (Color online) Intensity dependence of the light-induced field. The concentrations N_0 and N_1 are given in cm^{-3}.

4 corresponds to $N_0=10^{16}$ cm^{-3} and $N_1=10^{18}$ cm^{-3}; this models undoped SLN crystals. The limiting value of E_{pv} and the critical intensity are both relatively small in this case. The found regularities are in line with experiment.[21,36]

V. DISCUSSION

This study was strongly motivated by the latest experimental developments, especially by those relevant to the impact of stoichiometry on the photorefractive properties and optical-damage resistance of lithium niobate. It can be considered as an extension of the previous models—the one-center and two-center models developed for CLN crystals doped with Fe or Cu.

In contrast to the previous models,[8,15] we claim that the intermediate centers Nb_{Li} are important not only at high but also at low light intensities. Moreover, these centers provide, owing to their high concentration and not very strong electron localization, an additional channel of the charge transport. Simultaneously, the antisite defects play the central role in explaining the distinctive property of $LiNbO_3$ (and probably, $LiTaO_3$) crystals—the anomalously small values of the $\mu\tau$ product for the photoexcited charge carriers. This anomaly is naturally linked now with the structural peculiarity—the presence of a strong band of localized states not far from the conduction band.

Our model gives simple and explicit expressions for the light-induced field E_{pv} as a function of the concentrations of deep and intermediate centers $N_{0,1}$ and the light intensity I. Surprisingly, these expressions are in a reasonable qualitative agreement with experiment. Objective difficulties on the way of comparison with experiment are worth mentioning. (i) The concentration of the antisite defects N_1 is the quantity which is still difficult to vary and measure in the photorefractive experiments. (ii) The concentration of deep centers N_0 and the absorption coefficient α are usually unknown for nominally pure crystals. (iii) Only raw data on the optical damage are often available in the range of high intensities. Quantization of the relevant dependences is, most probably, the matter of time.

While our considerations of the electron migration over the intermediate centers are model dependent, they possess a

remarkable general feature. Both the mobility μ_1 and the recombination time τ_{10}^{-1} are proportional to the hopping probability $W_1(\bar{R}_1)$, so that the product $\mu_1\tau_{10}$, which determines the contribution of the intermediate centers to the photoconductivity, does not depend on this small and not very well-determined hopping parameter. This provides robustness for the model. Most probably, the use of more complicated hopping models will give modest modifications of the dependence of the photovoltaic field E_{pv} on N_0 and N_1.

Aiming at refining the concept from secondary details, we have restricted ourselves to the case of quasiuniform illumination which is relevant to the spot recording. An application to the case of grating recording can, however, be done straightforwardly, especially in the low-intensity and high-intensity ranges where effective one-center models are applicable. In particular, the photorefractive saturation field E_q is determined by the total electron concentration n_t and the grating vector K according to the conventional expression $E_q=en_t/\epsilon\epsilon_0 K$, where $\epsilon\epsilon_0$ is the static dielectric permittivity. In undoped crystals this field can become pretty low ($\lesssim E_{pv}$), causing energy transfer in two-wave coupling experiments.[39]

The restriction $I \ll \hbar\omega/\sigma_{12}\tau_{21}$ on the light intensity, which is valid within our model, can be too liberal because of very small values of τ_{21}. An additional restriction, $I \lesssim 10^9$ W/cm^2, comes from the influence of the two-photon band-band absorption and the instantaneous Kerr nonlinearity.[25,26] Anyhow, the intensity range where our model is expected to be applicable is very large.

Possibly, our model is applicable also to describe the influence of *optical-damage-resistant* dopants, such as Mg and Zn, on the photorefractive properties. It works if the role of these dopants is mainly in reducing concentration of the antisite defects. This scenario seems to be appropriate for sufficiently low doping levels.[21]

VI. CONCLUSIONS

We have proposed a conceptual model of light-induced charge transport for lithium niobate crystals, which are congruent or near stoichiometric. It incorporates some features of the known one-center and two-center models and includes additional important elements. (i) Fast recombination from the CB to the antisite defects (intermediate levels), (ii) negligible direct recombination to the deep traps, and (iii) additional channel of charge transport over the intermediate levels. In contrast to the previous models, the antisite defects become important even in the low-intensity region. The model explains the anomalously small values of the mobility-lifetime product for photoexcited electrons. It provides simple and explicit expressions for the light-induced field as a function of the concentrations of deep and intermediate centers and the light intensity. Being in line with experiment, these expressions are applicable in a wide range of these variable parameters.

ACKNOWLEDGMENTS

The authors are grateful to K. Buse for discussions and comments. This work was supported by the Spanish "Ministerio de Educacion y Cultura" under Grant No. MAT2005-06359-C03-01.

APPENDIX: RENORMALIZATION PROCEDURE

In the case of a nonmonoexponential relaxation, the product $\tau_{10}^{-1}n_1$ in Eqs. (1) and (2) has to be replaced by the general integral expression

$$\int_0^\infty n_1(t-t')f(t')dt'. \tag{A1}$$

The Laplace transforms n_{1p} and f_p are linked then by the relation $p+f_p=n_1(0)/n_{1p}$, where $n_1(0)$ is the initial value of $n_1(t)$. For $n_1(t)/n_1(0)=\exp[-(t/\tau_{10})^\beta]$, we have $f_0=1/q\tau_{10}$, where

$$q=\int_0^\infty \exp(-s^\beta)ds \tag{A2}$$

is a function of the stretching index β; it can easily be calculated numerically, see Fig. 2.

In steady state, expression (A1) transforms to

$$n_1\int_0^\infty f(t')dt' \equiv n_1 f_0 = n_1\tau_{10}^{-1}q^{-1}. \tag{A3}$$

Therefore, the time τ_{10} has to be replaced by the renormalized time $q\tau_{10}$ when calculating the steady-state values of $n_{0,1,2}$ from the balance Eqs. (1) and (2).

[1] A. Ashkin, G. D. Boyd, J. M. Dziedzic, R. J. Smith, A. A. Ballman, J. J. Levinstein, and K. Nassau, Appl. Phys. Lett. **9**, 72 (1966).
[2] A. M. Glass, D. von der Linde, and T. J. Negran, Appl. Phys. Lett. **25**, 233 (1974).
[3] L. Solymar, D. Webb, and A. Grunnet-Jepsen, *The Physics and Applications of Photorefractive Materials* (Clarendon, Oxford, 1996).
[4] L. E. Myers, R. C. Eckardt, M. M. Fejer, R. L. Byer, W. R. Bosenberg, and J. R. Pierce, J. Opt. Soc. Am. B **12**, 2102 (1995).
[5] Yu. S. Kuzminov, *Lithium Niobate Crystals* (Cambridge International Science Publishing, UK, 1999).
[6] L. Arizmendi, Phys. Status Solidi A **201**, 253 (2004).
[7] O. Caballero-Calero, A. Garcia-Cabañes, J. M. Cabrera, and M. A. Alcazar, J. Appl. Phys. **100**, 093103 (2006).
[8] E. Krätzig and O. F. Schirmer, in *Photorefractive Centers in Electro-optic Crystals*, edited by P. Günter and J.-P. Huignard, Topics in Applied Physics: Photorefractive Materials and Their Applications I Vol. 61 (Springer-Verlag, Berlin, 1988).

[9] P. Günter and J.-P. Huignard, in *Photorefractive Effects and Materials*, edited by P. Günter and J.-P. Huignard, Topics in Applied Physics: Photorefractive Materials and Their Applications I Vol. 61 (Springer-Verlag, Berlin, 1988).
[10] V. Fridkin and B. Sturman, *The Photovoltaic and Photorefractive Effects in Noncentrosymmetric Materials* (Gordon and Breach, New York, 1992).
[11] B. Sturman, J. Opt. Soc. Am. B **8**, 1333 (1991).
[12] R. E. Peierls, *Quantum Theory of Solids* (Clarendon, Oxford, 1955).
[13] K. Seeger, *Semiconductor Physics* (Springer, New York, 1973).
[14] A. Othonos, J. Appl. Phys. **83**, 1789 (1998).
[15] F. Jermann and J. Otten, J. Opt. Soc. Am. B **10**, 2085 (1993).
[16] J. Carnicero, O. Caballero, M. Carrascosa, and J. M. Cabrera, Appl. Phys. B: Lasers Opt. **79**, 351 (2004).
[17] M. Carrascosa, J. Villarroel, J. Carnicero, A. Garcia-Cabanes, and J. M. Cabrera, Opt. Express **16**, 115 (2008).
[18] *Properties of Lithium Niobate*, edited by K. K. Wong, EMIS Datareview Series Vol. 28 (INSPEC, London, 2002).
[19] A. Briat, V. G. Grachev, G. I. Malovichko, O. F. Schirmer, and M. Wöhlecke, in *Photorefractive Materials and Their Applications 2*, edited by P. Günter and J.-P. Huignard (Springer, New York, 2007).
[20] H. Hatana, Y. Liu, and K. Kitamura, in *Photorefractive Materials and Their Applications 2*, edited by P. Günter and J.-P. Huignard (Springer, New York, 2007).
[21] T. Volk, M. Wöhlecke, and N. Rubinina, in *Photorefractive Materials and Their Applications 2*, edited by P. Günter and J.-P. Huignard (Springer, New York, 2007).
[22] D. Berben, K. Buse, S. Wevering, P. Herth, M. Imlau, and Th. Woike, J. Appl. Phys. **87**, 1034 (2000).
[23] P. Herth, D. Schaniel, Th. Woike, T. Granzow, M. Imlau, and E. Krätzig, Phys. Rev. B **71**, 125128 (2005).
[24] Y. S. Bai and R. Kachru, Phys. Rev. Lett. **78**, 2944 (1997).
[25] O. Beyer, D. Maxein, K. Buse, B. Sturman, H. T. Hsieh, and D. Psaltis, Phys. Rev. E **71**, 056603 (2005).
[26] B. Sturman, O. Beyer, D. Maxein, and K. Buse, J. Opt. Soc. Am. B **24**, 419 (2007).
[27] P. Reckenthaeler, D. Maxein, Th. Woike, K. Buse, and B. Sturman, Phys. Rev. B **76**, 195117 (2007).
[28] J. Carnicero, M. Carrascosa, G. Garcia, and F. Agullo-Lopez, Phys. Rev. B **72**, 245108 (2005).
[29] V. I. Gol'danskii, L. I. Trakhtenberg, and V. N. Flerov, *Tunneling Phenomena in Chemical Physics* (Gordon and Breach, New York, 1989).
[30] B. Sturman, E. Podivilov, and M. Gorkunov, Phys. Rev. Lett. **91**, 176602 (2003).
[31] B. I. Shklovskii and A. L. Efros, *Electronic Properties of Doped Semiconductors* (Springer, New York, 1984).
[32] I. Nee, M. Müller, K. Buse, and E. Krätzig, J. Appl. Phys. **88**, 4282 (2000).
[33] K. Buse, J. Imbrock, E. Krätzig, and K. Peithmann, in *Photorefractive Materials and Their Applications 2*, edited by P. Günter and J.-P. Huignard (Springer, New York, 2007).
[34] K. Peithmann, A. Wiebrock, and K. Buse, Appl. Phys. B: Lasers Opt. **68**, 777 (1999).
[35] G. I. Malovichko, V. Grachev, E. Kokonyan, O. Schirmer, K. Betzler, B. Gather, F. Jermann, S. Klauer, U. Schlarb, and M. Wöhlecke, Appl. Phys. A: Solids Surf. **56**, 103 (1993).
[36] F. Jermann, M. Simon, and E. Krätzig, J. Opt. Soc. Am. B **12**, 2066 (1995).
[37] M. Fontana, K. Chah, M. Aillerie, R. Mouras, and P. Bourson, Opt. Mater. **16**, 111 (2001).
[38] Y. Furukawa, M. Sato, K. Kitamura, Y. Yajima, and M. Minakata, J. Appl. Phys. **72**, 3250 (1992).
[39] X. Chen, B. Li, J. Xu, D. Zhu, S. Pan, and Z. Wu, J. Appl. Phys. **90**, 1516 (2001).